

Article

Effects of Emulsion-Based Resonant Infrared Matrix Assisted Pulsed Laser Evaporation (RIR-MAPLE) on the Molecular Weight of Polymers

Ryan D. McCormick ¹, Jeremy Lenhardt ² and Adrienne D. Stiff-Roberts ^{1,*}

¹ Department of Electrical and Computer Engineering, Duke University, Durham, NC 27708, USA; E-Mail: ryan.mccormick@duke.edu

² Department of Chemistry, Duke University, Durham, NC 27708, USA; E-Mail: jlenhardt@gmail.com

* Author to whom correspondence should be addressed; E-Mail: adrienne.stiffroberts@duke.edu; Tel.: +1-919-660-5560.

Received: 31 December 2011; in revised form: 29 January 2012 / Accepted: 30 January 2012 / Published: 1 February 2012

Abstract: The molecular weight of a polymer determines key optoelectronic device characteristics, such as internal morphology and charge transport. Therefore, it is important to ensure that polymer deposition techniques do not significantly alter the native polymer molecular weight. This work addresses polymers deposited by resonant infrared matrix-assisted pulsed laser evaporation (RIR-MAPLE). By using a novel emulsion-based target technique, the deposition of smooth, contiguous films with no evidence of chemical degradation have been enabled. However, structural degradation via a reduction in molecular weight remains an open question. The common polymer standard, PMMA, and the optoelectronic polymers, P3HT and MEH-PPV, have been characterized before and after emulsion-based RIR-MAPLE deposition via gel permeation chromatography to determine if RIR-MAPLE affects the deposited polymer molecular weight. Proton nuclear magnetic resonance spectroscopy and Fourier transform infrared spectroscopy measurements have also been conducted to verify the absence of chemical degradation. These measurements verify that there is no chemical degradation of the polymers, and that PMMA and P3HT show no structural degradation, but MEH-PPV exhibits a halving of the weight-averaged molecular weight after RIR-MAPLE deposition. Compared with competing laser deposition techniques, RIR-MAPLE is shown to have the least effect on the molecular weight of the resulting thin films.

Keywords: RIR-MAPLE; molecular weight; gel permeation chromatography

1. Introduction

The molecular weight of a conjugated polymer plays a central role in the optoelectronic properties of conjugated polymer thin films. Properties such as absorption, carrier mobilities, charge transport, and device efficiency are sensitive to chromophore length and polymer chain-packing morphology, which in turn depend on the preparation conditions and the molecular weight of the polymer [1]. For example, it has been demonstrated that larger molecular weight poly(3-hexylthiophene) (P3HT) films lead to larger carrier mobilities and red-shifted absorption spectra in organic field-effect transistors [2,3] and organic photovoltaic solar cells [4] compared with lower molecular weight samples. Organic light-emitting diodes have shown increased electroluminescence intensities and better spectral stability at higher molecular weights [5]. The larger molecular weight improves charge transport by packing the chains more closely, which increases π - π orbital interactions, and by linking otherwise isolated crystalline domains for better hopping transport. Therefore, it is important that the use of a given deposition technique does not structurally degrade the polymer.

Various polymer deposition techniques, such as spin-casting, drop-casting, ink-jet printing, and pulsed laser deposition (PLD) suffer from a lack of morphology control. However, emulsion-based resonant infrared matrix-assisted pulsed laser evaporation (RIR-MAPLE) is a promising deposition technology for the fabrication of polymer-based optoelectronic devices for two primary reasons: (i) the ability to control film morphology; and (ii) the ability to deposit multi-layered heterostructures [6–10]. The novelty of the emulsion-based RIR-MAPLE approach, compared to alternative MAPLE implementations [11–18], is that the ideal growth regime, *i.e.*, strong laser absorption by the host matrix and little to no laser absorption by the guest material, can be achieved for almost any polymer, even though most polymers of interest and many compatible solvents do not resonantly absorb the Er:YAG laser energy at 2.94 μm . This challenge is overcome due to the target emulsion in which a secondary solvent and deionized water, both rich in O-H bonds that are resonant with the Er:YAG laser energy, are added to the polymer solution. However, it is important to determine whether the emulsion-based RIR-MAPLE structurally degrades the deposited polymers. A variety of pulsed laser deposition and MAPLE techniques have yielded polymer films for which the chemical integrity remains intact, as characterized by proton nuclear magnetic resonance (^1H NMR) and Fourier transform infrared (FTIR) spectroscopies. However, gel permeation chromatography (GPC) measurement of the structural integrity of the polymers often finds a reduction in molecular weight after deposition [12,13,19–21].

In this paper, the effects of the emulsion-based RIR-MAPLE thin film deposition technique on polymer molecular weight are presented. Poly(methyl methacrylate) (PMMA) is included in the study as a standard reference due to the availability of sharply peaked size distributions over a wide range of molecular weights. A unique aspect of this work is that the molecular weight for polymers that are important for optoelectronic devices are characterized by GPC measurement: P3HT, which is widely used in organic photovoltaics and organic transistors; and,

poly[2-methoxy-5-(2'-ethyl-hexyloxy)-p-phenylene-vinylene] (MEH-PPV), which has been an important polymer in the development of organic light-emitting diodes and organic photovoltaics. The molecular weight of each polymer is determined by GPC both before and after deposition by emulsion-based RIR-MAPLE. A survey of the literature yielded several published values of the molecular weight of laser-deposited polymer films. These results are compiled for comparison with the present work. Complementary characterizations by ^1H NMR spectroscopy and FTIR spectroscopy provide information on the chemistry of the polymers.

2. Results and Discussion

2.1. GPC Measurement of Polymer Molecular Weight

GPC measurements provide information on the size distribution of observed particles, and are sensitive to a number of parameters. The use of light scattering to determine molecular weight is best suited to spherical particles. As the particle shape deviates from a sphere, as it does with linear polymers, there will be an error introduced into the measurement [22]. It is well-known that molecular weight measurements of rigid backbone polymers, taken on a GPC system that has been calibrated with polystyrene standards, tend to overestimate the true weight-averaged molecular weight (M_w) values. However, relative measurements, such as those reported here, minimize such biases due to the identical offset introduced throughout a data set. Similarly, reported values of the refractive index increment dn/dc of a given polymer tend to be inconsistent. Because the increment affects different samples of the same material equally, any systematic error present is eliminated with a relative comparison. Thus, the *change* in molecular weight, denoted “ M_w % Change”, from the RIR-MAPLE deposited polymer relative to the native polymer is reported. A positive value indicates an increase in M_w after deposition, while a negative value indicates a decrease. The measured molecular weight values, both from existing literature and the current work, are presented in Table 1.

Bubb *et al.*, used RIR-PLD to deposit the copolymer poly(lactide-*co*-glycolide) (PLGA) for a drug delivery coating application [13]. GPC measurements indicated the molecular weight of the polymer was less than half that of the native polymer. Mercado *et al.*, explicitly compared thin films of PLGA deposited by UV-PLD and UV-MAPLE [19]. A molecular weight distribution analysis via GPC revealed significant differences between the native and deposited polymers for both deposition techniques. Bubb *et al.* also used UV-MAPLE depositions of polyethylene glycol (PEG) to establish that the solvent plays an important role in determining the level of structural degradation, with DI water yielding less structural degradation of the polymer compared to chloroform [12]. It was concluded that chloroform yielded chemically reactive chloride species during deposition that were responsible for structural degradation of the polymer, while water did not photodissociate into reactive species and did not generate structural changes in the polymer to the same extent. Fitz-Gerald *et al.*, reported on the UV-MAPLE deposition of a Ruthenium-based PMMA polymeric metal complex [20]. A low-MW peak in the size distribution indicated partial cleavage of the PMMA chains. Sellinger *et al.*, looked at a nanocomposite of carbon nanotubes embedded within a PMMA matrix [21]. GPC analysis revealed a molecular weight reduction of the PMMA, most likely due to the polymer absorption of UV light.

Table 1. Molecular weight of polymers deposited by PLD, UV-MAPLE and RIR-MAPLE. Values from this work are averages of multiple samples. M_w % Change indicates the change in M_w after deposition relative to the native polymer. (* M_n —number-averaged molecular weight).

Author	Polymer	Solvent	Method	Laser λ (nm)	Native M_w (kDa)	Deposited M_w (kDa)	M_w % Change
Bubb [13]	PLGA	-	RIR-PLD	2940	8.495	3.125	-63.2
Bubb [13]	PLGA	-	RIR-PLD	3400	8.495	3.470	-59.2
Mercado [19]	PLGA	-	UV-PLD	248	99	8	-91.9
Mercado [19]	PLGA	Chloroform	UV-MAPLE	248	99	26	-73.7
Bubb [12]	PEG	DI Water	UV-MAPLE	193	1.397	1.325	-5.2
Bubb [12]	PEG	Chloroform	UV-MAPLE	193	1.397	1.077	-22.9
Fitz-Gerald [20]	[Ru(bpyPMMA ₂) ₃] -(PF ₆) ₂	Dimethoxyethane	UV-MAPLE	248	*33.0	*9–12	-68.2
Sellinger [21]	PMMA	Toluene	UV-MAPLE	248	13.9	12.8	-7.9
McCormick	PMMA	TCE/BnOH/H ₂ O	RIR-MAPLE	2940	9.57	11.2	3.3
McCormick	PMMA	TCE/BnOH/H ₂ O	RIR-MAPLE	2940	109.4	117.0	6.9
McCormick	PMMA	TCE/BnOH/H ₂ O	RIR-MAPLE	2940	367.2	354.2	-3.5
McCormick	P3HT	TCE/Phenol/H ₂ O	RIR-MAPLE	2940	42.5	45.3	6.6
McCormick	MEH-PPV	Toluene/Phenol/H ₂ O	RIR-MAPLE	2940	266.9	133.7	-49.9

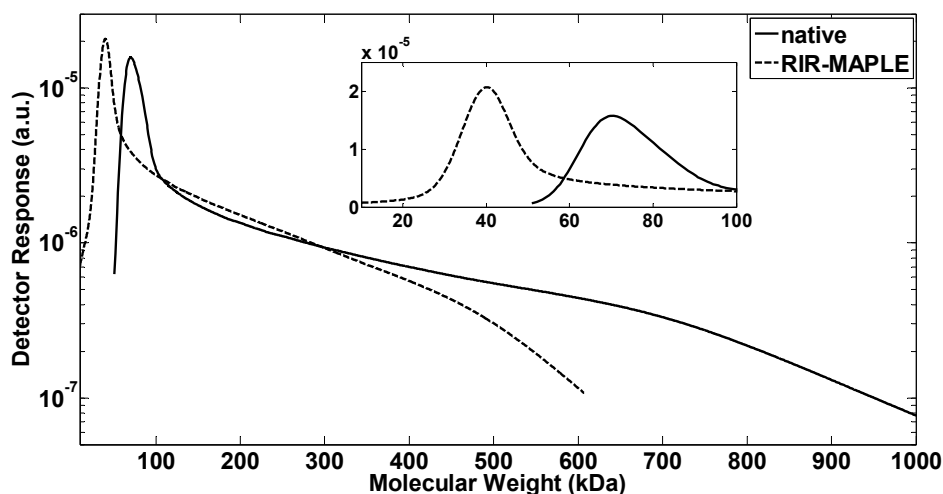
From this existing work, a few trends can be observed. The PLD films all exhibited significant M_w degradation regardless of laser wavelength, which is to be expected because the target consists of solid polymer, which must absorb the laser energy to desorb material for deposition. The UV-MAPLE films also exhibited degradation compared with the native polymer. Total degradation of the UV-MAPLE process may be due both to direct light absorption by the polymer and to chemical degradation of the polymer from highly reactive species created via photodissociation of the solvent [12]. Overall, it is clear that RIR- and UV-PLD techniques cause significant structural degradation of the deposited polymer. Likewise, UV-MAPLE results in a global reduction of molecular weight, although the extent of the molecular weight degradation can be minimized.

In contrast, the emulsion-based RIR-MAPLE depositions shown in Table 1 show the least amount of structural degradation because the solvent emulsion is responsible for the majority of the IR laser light absorption at the hydroxyl bond stretch; the polymer absorbs very poorly in this wavelength regime. The PMMA polymer provides a good example of this fundamental difference as it can be compared directly to other laser deposition techniques represented in Table 1. Three different PMMA molecular weights, $M_w = 10$ kDa, 100 kDa, and 350 kDa, were chosen to span a range representative of polymers. Wyatt Technology reports a 5% system error for the molecular weight measurement, which encompasses the light scattering and refractive index measurements. The weight-averaged molecular weight, M_w , of the 10 kDa and 100 kDa PMMA samples demonstrate an increase in the molecular weight that deviates from the native values by less than or slightly more than, respectively, the reported system error. The 350 kDa PMMA sample demonstrated a molecular weight reduction of 3.5%, which is within the system error. Therefore, the GPC distributions of the PMMA standards

reflect a negligible change of the RIR-MAPLE-deposited material from the native polymer. These results also demonstrate that emulsion-based RIR-MAPLE does not have an inherent molecular weight limit, within the 10–350 kDa range, to prevent a polymer from being deposited intact. It is important to note that the PEG sample in Table 1 that was deposited by UV-MAPLE and had a 5.2% decrease in M_w [12], used DI water as the target solvent. The RIR-MAPLE emulsion technique features DI water as a major portion of the target matrix.

In the case of P3HT, the RIR-MAPLE deposited sample increased in molecular weight compared with the native sample. Sigma-Aldrich reported the native polymer molecular weight as $M_w = 42.5$ kDa, which corresponds to a 6.6% increase for the RIR-MAPLE-deposited samples, as shown in Table 1. While it is well-known that P3HT cross-linking is the preferred mechanism (as opposed to chain scission) in the presence of air and UV or visible light [23], it is unlikely that cross-linking would occur to such a degree given that the polymer samples were kept in light-shielded cases under vacuum. Such significant cross-linking would lead to a loss of solubility, which was not observed.

Figure 1. GPC measurements of the native MEH-PPV polymer and the resulting distributions after RIR-MAPLE deposition. The log-scale plot emphasizes the reduction in the largest molecular weights after MAPLE deposition. The inset shows the peak values on a linear scale. These distributions are representative of repeated GPC measurements.



Only MEH-PPV exhibited structural degradation after RIR-MAPLE deposition, with a consistent halving of the weight-averaged molecular weight. Figure 1 shows the GPC traces of single representative MEH-PPV samples before and after deposition by emulsion-based RIR-MAPLE. Because the distribution is skewed, the data are plotted on a log-scale plot to emphasize the higher molecular weight tails. The inset clearly shows a shift of the peak value from 70 kDa to 40 kDa in the RIR-MAPLE deposited sample. Furthermore, it is evident from the high molecular weight tails that there is a reduction of the highest molecular weights present in the two samples: the native sample has molecular weights up to 1 MDa, while the sample after RIR-MAPLE deposition has maximum molecular weight values of 600 kDa. Analysis of PMMA with nominal $M_w = 350$ kDa, which is roughly 100 kDa larger than the MEH-PPV native polymer, showed that there was no change in the PMMA molecular weight after RIR-MAPLE deposition. Therefore, even if an upper limit to the deposition capabilities of RIR-MAPLE does exist with respect to the molecular weight, MEH-PPV

should be well below that limit. In fact, Figure 1 shows that the MEH-PPV sample after deposition by RIR-MAPLE has molecular weight values as high as 600 kDa.

At this point, it is also helpful to consider the polydispersity index (PDI) for the polymers described in Table 1. The PDI is defined as the ratio of the weight-averaged to the number-averaged molecular weights (M_w/M_n), and it provides an indication of how uniformly the molecular weight is distributed in a polymer sample, with a value of unity marking a monodisperse, narrow, highly-peaked size distribution. As the PDI increases past unity, the size distribution becomes less uniform, broader, and less peaked. Table 2 reports the PDI of the polymers described in Table 1. The RIR- and UV-PLD samples showed an increase of 57–150 % of the native PDI, signifying a large increase in the number of different molecular weight values after deposition. In contrast, both UV-MAPLE and RIR-MAPLE have much smaller changes in PDI. The UV-MAPLE technique had PDI changes after deposition ranging from an 11% decrease to a 16% increase compared to the native PDI. The PDI of RIR-MAPLE-deposited polymers ranged from a 7% decrease to a 10% increase compared to the native PDI. Therefore, even if the GPC size distribution shifts to a different M_w value after deposition using MAPLE techniques, the distribution of the molecular weight values remains relatively constant.

Table 2. Polydispersity index (PDI) of polymers deposited by PLD, UV-MAPLE and RIR-MAPLE (* PDI not reported).

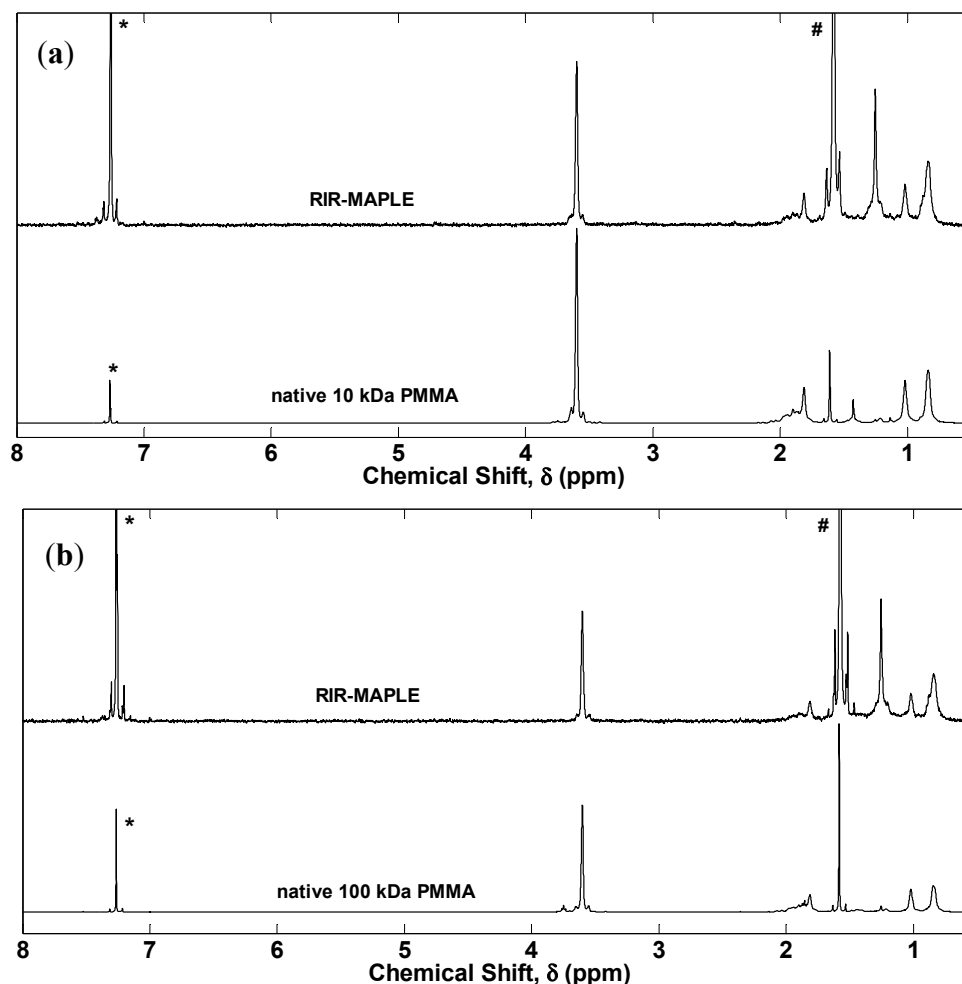
Author	Polymer	Solvent	Method	Laser λ (nm)	Native PDI	Deposited PDI
Bubb [13]	PLGA	-	RIR-PLD	2940	1.22	3.05
Bubb [13]	PLGA	-	RIR-PLD	3400	1.22	2.63
Mercado [19]	PLGA	-	UV-PLD	248	1.73	2.70
Mercado [19]	PLGA	Chloroform	UV-MAPLE	248	1.73	2.00
Bubb [12]	PEG	DI Water	UV-MAPLE	193	1.02	1.06
Bubb [12]	PEG	Chloroform	UV-MAPLE	193	1.02	1.07
Fitz-Gerald [20]	[Ru(bpyPMMA ₂) ₃](PF ₆) ₂	Dimethoxyethane	UV-MAPLE	248	*	*
Sellinger [21]	PMMA	Toluene	UV-MAPLE	248	1.71	1.53
McCormick	PMMA	TCE/BnOH/H ₂ O	RIR-MAPLE	2940	1.12	1.04
McCormick	PMMA	TCE/BnOH/H ₂ O	RIR-MAPLE	2940	1.15	1.19
McCormick	PMMA	TCE/BnOH/H ₂ O	RIR-MAPLE	2940	1.45	1.59
McCormick	P3HT	TCE/Phenol/H ₂ O	RIR-MAPLE	2940	2.20	2.04
McCormick	MEH-PPV	Toluene/Phenol/H ₂ O	RIR-MAPLE	2940	2.29	2.18

2.1. ¹H NMR Spectroscopy and FTIR Spectroscopy of Polymers Deposited by RIR-MAPLE

In order to determine if the observed change in molecular weight for MEH-PPV results from RIR-MAPLE deposition alone, or from a separate mechanism, such as chain scission, ¹H NMR and FTIR spectra were measured for PMMA, P3HT, and MEH-PPV before and after deposition by emulsion-based RIR-MAPLE. The ¹H NMR spectra of PMMA confirm the GPC results by reporting no change before and after RIR-MAPLE deposition, as shown in Figure 2. FTIR spectra are not reported for the PMMA samples due to the definitive and uneventful results of the other characterizations. The PMMA results represent a baseline for the other polymers applicable to

optoelectronic devices by demonstrating that the RIR-MAPLE technique is capable of thin film deposition with little to no change in the native polymer within the wide range of 10–350 kDa.

Figure 2. Proton NMR spectra of PMMA of molecular weight (a) 10 kDa, and (b) 100 kDa. The solvent peak at $\delta = 7.26$ ppm is denoted by *. The water peak at $\delta = 1.56$ ppm is denoted by #.



The P3HT ^1H NMR spectra, shown in Figure 3, were slightly more complex. There was a small reduction in the thiophene proton peak near $\delta = 7$ ppm and changes in the amplitude, but not position, of the alkyl side group peaks. Integration of the α -carbon proton peaks in the region $\delta = 3.0$ – 2.5 ppm yielded a regioregularity of $\sim 92\%$ [24], which agrees with the manufacturer specification of $>90\%$ regioregularity. The primary difference before and after RIR-MAPLE deposition is the sharp increase in the CH_2 peak at $\delta = 1.26$ ppm, which could indicate that the side chain has been shortened from six to five alkyl units. This shortening is not great enough to lead to an appreciable difference in solubility; moreover, a solubility difference was not observed. The P3HT FTIR spectra in Figure 4 contain the requisite peaks both before and after RIR-MAPLE with no significant differences. Following Chen *et al.*, the observed peaks are assigned as [25]: the aromatic C–H stretch near $3,057\text{ cm}^{-1}$; the aliphatic C–H stretches at $2,954$, $2,925$ and $2,856\text{ cm}^{-1}$; the ring stretches at $1,510$ and $1,454\text{ cm}^{-1}$; the methyl deformation at $1,377\text{ cm}^{-1}$; the out-of-plane aromatic stretches at 820 cm^{-1} ; and, the methyl rocking stretch at 725 cm^{-1} .

Figure 3. Proton NMR spectra of native P3HT polymer and RIR-MAPLE deposited samples. The solvent peak at $\delta = 7.26$ ppm is denoted by *. The water peak at $\delta = 1.56$ ppm is denoted by #.

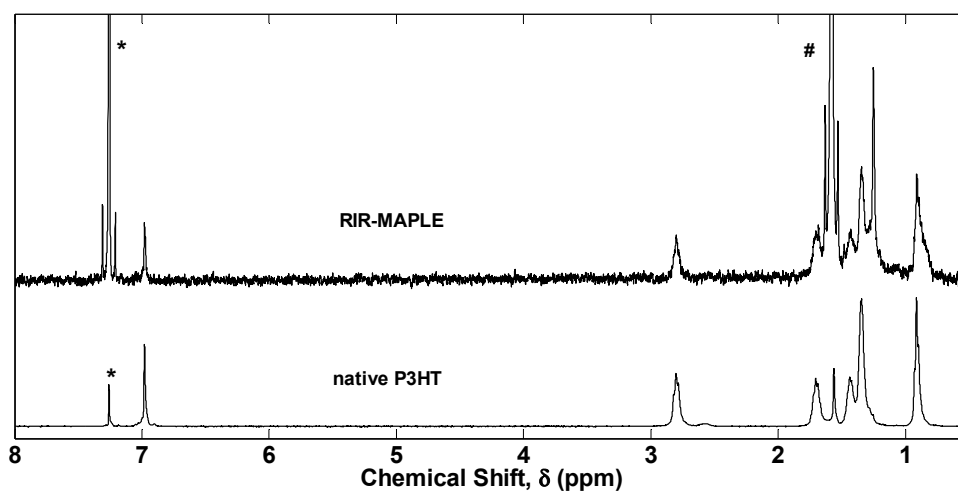
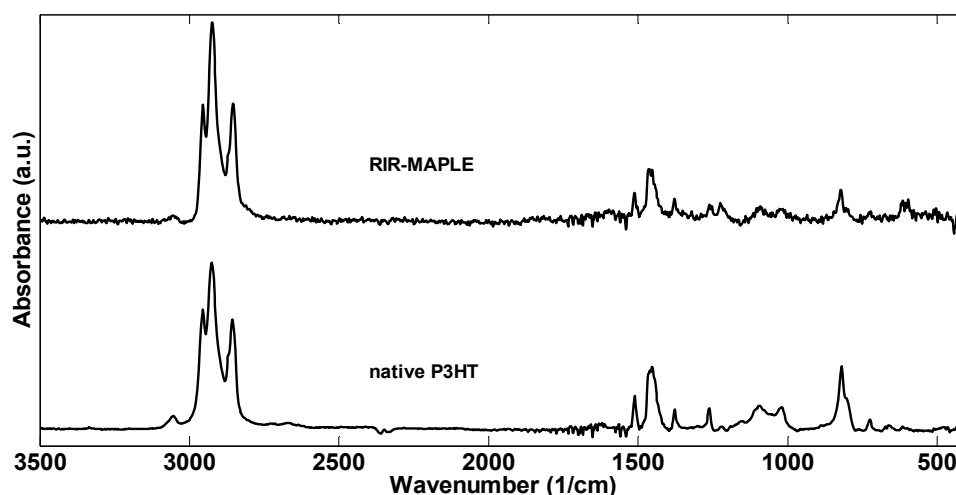


Figure 4. FTIR spectra of P3HT before and after RIR-MAPLE deposition.



The MEH-PPV ^1H NMR spectra, shown in Figure 5, contain marked differences before and after RIR-MAPLE deposition. The aliphatic solvent chloroform- d (CDCl_3), which tends to dissolve the alkyl side chains better than the aromatic backbone, was used for sample preparation [26]. MEH-PPV is a well-studied polymer with a ^1H NMR spectrum that has been extensively catalogued [27–29]. There are three regions of interest in the MEH-PPV spectrum: the downfield aromatic groups ($\delta = 7.55\text{--}7.45$ ppm, ArH) and vinyl double bonds of the backbone ($\delta = 7.23\text{--}7.12$ ppm, vinyl HC=CH); the midfield alkoxy groups ($\delta = 3.95, 3.92$ ppm, $\text{OCH}_2, \text{OCH}_3$); and finally, the upfield alkyl side chains ($\delta = 1.81, 1.65, 1.60, 1.55, 1.35, 1.24$ ppm, CH, CH_2), (1.02, 0.99, 0.97; 0.92, 0.90, 0.88 ppm, CH_3). The aromatic peaks remained constant in both location and magnitude, indicating that the benzene ring in the polymer backbone remained intact. The vinyl double bond peaks decreased after RIR-MAPLE, indicating a decrease in the number of these bonds, which supports the chain scission seen in the molecular weight distributions. The side chain peaks were dramatically different before and after RIR-MAPLE. The peaks corresponding to the CH and CH_2 groups in the $\delta = 1.88\text{--}1.40$ ppm region broadened significantly, and resulted in a complete loss of structure. If

chemical degradation had occurred, the broad peak would be an indicator of a multitude of different alkyl products [30]. However, as demonstrated by the FTIR spectra to follow, such chemical degradation does not occur. The CH₂ peak at $\delta = 1.35$ ppm remained constant, while there was an increase in the CH₂ peak at $\delta = 1.24$ ppm. The methyl groups in the $\delta = 1.02$ – 0.88 ppm region were intact, but the grouping at $\delta = 0.92$ – 0.88 ppm exhibited a broadening to $\delta = 0.92$ – 0.81 ppm. All of these changes in the ¹H NMR spectra demonstrate substantial modification of the side chains after deposition by emulsion-based RIR-MAPLE. The solubility of the polymer would be impacted if the side chain modification is severe or leads to complete removal. Yet, the MEH-PPV solubility was not significantly changed after RIR-MAPLE because dissolution of the polymers for ¹H NMR & GPC analysis was still possible. However, substantial modification of the side chains could potentially lead to changes in the morphology of the deposited film due to altered interchain interactions and chain stacking, which would affect device properties such as carrier mobility and efficient exciton dissociation.

Figure 5. Proton NMR spectra of native MEH-PPV and of MEH-PPV after RIR-MAPLE deposition. The solvent peak is denoted by *.

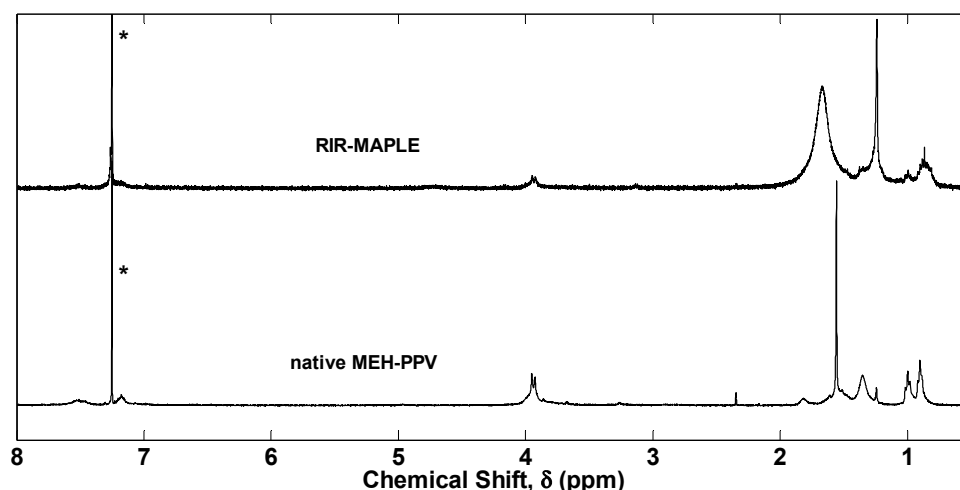
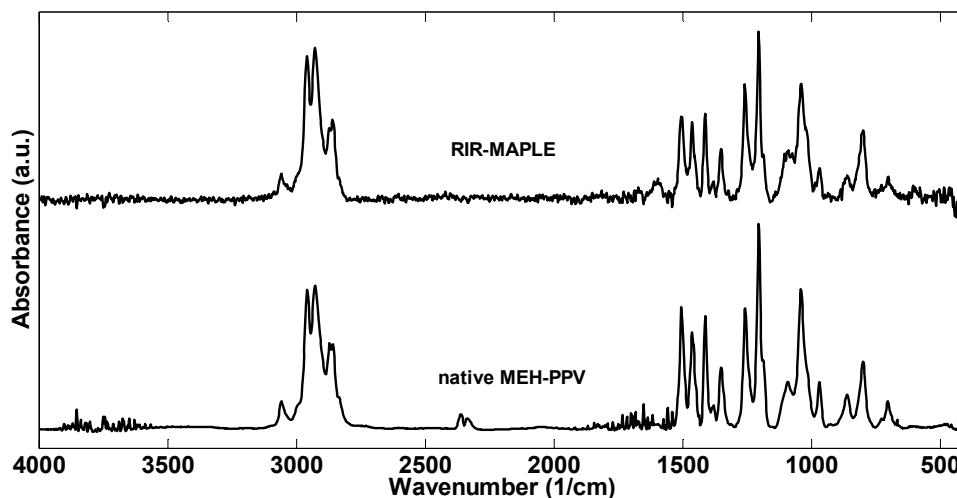


Figure 6 shows the FTIR spectra for MEH-PPV. The peak assignments follow Ram *et al.* [27]: $3,058\text{ cm}^{-1}$ is the CH vinyl bond stretch; $2,958\text{ cm}^{-1}$ is the CH₃ alkyl stretch; $2,928\text{ cm}^{-1}$ is the CH alkyl stretch; $2,858$ and $2,872$ are the CH₂ alkyl stretch; $1,600$, $1,506$, $1,464$ and $1,413\text{ cm}^{-1}$ are various phenyl stretches; $1,351\text{ cm}^{-1}$ is the CH₂ alkyl deformation; $1,259$ and $1,205\text{ cm}^{-1}$ are the phenyl oxygen stretches; $1,041\text{ cm}^{-1}$ is the alkyl oxygen stretch; and 969 cm^{-1} is the vinyl CH wag. From these FTIR spectra, there appears to be no change in the chemical bonds of MEH-PPV due to RIR-MAPLE. The FTIR and ¹H NMR results are not contradictory. Because ¹H NMR probes chemical bonds and their local magnetic environment, it is possible to demonstrate no change in the specific bonds present via FTIR and also to find differences in the ¹H NMR spectra due to structural changes in the polymer.

Figure 6. FTIR spectra of MEH-PPV. There is no difference between the native polymer and the RIR-MAPLE deposited polymer.



3. Experimental Section

All polymers were used as-received from the manufacturer. All molecular weights of the PMMA and the P3HT (>90% regioregularity) polymers were purchased from Sigma-Aldrich. The MEH-PPV was purchased from American Dye Source. All samples were deposited by emulsion-based RIR-MAPLE onto soda-lime glass slides, except for the FTIR samples, which were deposited onto undoped silicon. In the RIR-MAPLE deposition process, the prepared polymer emulsion is flash frozen in a target cup that has been cooled to 77 K by liquid nitrogen. The flash freezing process solidifies the emulsion before it is able to separate, which allows materials of disparate solubilities to be deposited. There are two primary advantages to having the target and substrate located in a vacuum chamber. First, in order to avoid liquid contamination of the deposited film, a lower environmental pressure allows the target material to sublime so that the vaporous solvent can be pumped away by the vacuum system. Second, the plume of ablated target material forms more evenly under vacuum. In the vacuum chamber, a substrate is located facing the target and rotates during a deposition. A 2-Hz pulsed Er:YAG laser (2.94 μm) rasters across the rotating target in a pattern that ensures the target is ablated evenly. The absorption peaks of the polymers occur within the visible wavelength range; therefore, the majority of the laser absorption occurs in the solvent, leaving the polymer minimally affected. The RIR-MAPLE parameters were standardized across depositions to the following values: a target-to-substrate distance of 70 mm; an ambient chamber pressure of $1\text{E}-5$ – $1\text{E}-4$ Torr; and, a substrate temperature of 4 °C. The targets consisted of emulsions of multiple solvents, in contrast with traditional solution casting, which generally uses a single solvent. PMMA was prepared as a 1 wt% solution in trichloroethylene (TCE) as the primary solvent, to which benzyl alcohol (BnOH) was added as a secondary solvent. Deionized (DI) water was then added in a 2:1 water:solution weight ratio to complete the emulsion. The P3HT emulsion target was prepared using the same polymer/solvent/DI water ratios, with TCE as the primary solvent and phenol as the secondary solvent. Finally, MEH-PPV was prepared using the same ratios, with toluene as the primary solvent and phenol as the secondary solvent.

The polymer films deposited by RIR-MAPLE onto glass slides were prepared for GPC measurements by dissolution in tetrahydrofuran (THF) and then by isolating the polymer for molecular weight measurement using standard rotary evaporator techniques. Clean THF was mixed with the polymer in an amount to achieve 2 mg/mL for GPC analysis. Only 200 μ L of the polymer solution was injected into the GPC system to reduce peak broadening. GPC analysis was carried out on the following equipment: Optilab DSP Interferometric Refractometer and Dawn EOS—Enhanced Optical System, both from Wyatt Technology. The polymer was separated in a PLgel, 5 μ m, 10^4 Å column from Agilent Technologies, using inhibitor-free THF as the mobile phase. The system was able to measure an approximate range of the M_w between 10^4 – 10^6 g/mol (Da) with a light scattering wavelength of $\lambda = 690$ nm. ASTRA V software, version 5.3.4.16 (Wyatt Technology), was used for data analysis. The values of the refractive index increment, dn/dc , using THF as the mobile phase were determined after injecting a known amount of polymer: PMMA $dn/dc = 0.088$ [31], P3HT $dn/dc = 0.285$ [32], and MEH-PPV $dn/dc = 0.293$; when possible, these values have been confirmed from the literature. GPC samples were measured within one day after removal from vacuum.

^1H NMR spectra were taken on a Varian Inova 400 MHz spectrometer. Sample preparation took place in a chemical fume hood. Samples were dissolved in chloroform- d and injected into Wilmad-LabGlass Pyrex 5 mm tubes for testing. Final spectra were an average of 64 runs on samples that were exposed to atmosphere for less than one day. FTIR spectra were taken on a Thermo Electron Nicolet 8700 spectrometer with 1.9 cm^{-1} wavenumber resolution. The films had been deposited onto undoped silicon and were measured in transmission mode under a nitrogen atmosphere at room temperature. All RIR-MAPLE films were measured by FTIR within one hour of removal from the vacuum system. Until ready for measurement, samples were kept in plastic clamshell cases that were wrapped in aluminum foil to shield them from ambient light. The P3HT and MEH-PPV samples were characterized by FTIR within one hour of deposition in order to minimize contact both with the atmosphere and with light sources.

4. Conclusions

PMMA, P3HT and MEH-PPV were characterized by GPC, ^1H NMR and FTIR both before and after RIR-MAPLE deposition to determine if RIR-MAPLE had an effect on the molecular weight. Three molecular weights of a PMMA standard spanned the range $M_w = 10$ – 350 kDa and showed no decrease in molecular weight after RIR-MAPLE deposition. If RIR-MAPLE has an inherent limit to the molecular weight that can be deposited without degradation, it is outside of the range defined by the PMMA depositions. P3HT showed no change in molecular weight. MEH-PPV experienced a halving of the molecular weight after RIR-MAPLE deposition. The ^1H NMR results imply a reduction of the vinyl double bonds along the backbone, which corroborates the observed molecular weight reduction due to scission. In addition, the side chains are still present, although in altered form. All polymers maintained their solubility characteristics. There is no evidence for photo-oxidative degradation of MEH-PPV, indicating that the observed effects are due to the RIR-MAPLE deposition. However, PLD, which has a M_w degradation range of 50–90%, and UV-MAPLE, which has a degradation range of 5–74%, causes more damage to deposited polymers. Therefore, this work

establishes that, of the laser deposition techniques, emulsion-based RIR-MAPLE has the least effect on the molecular weight of the deposited polymers.

Acknowledgments

This work was supported by the Office of Naval Research under Grant N00014-10-1-0481. The authors would also like to thank Stephen Craig of Duke University for his kind assistance in the performance of the GPC experiments.

References

1. Chochos, C.L.; Choulis, S.A. How the structural deviations on the backbone of conjugated polymers influence their optoelectronic properties and photovoltaic performance. *Prog. Polym. Sci.* **2011**, *36*, 1326–1414.
2. Kline, R.J.; McGehee, M.D.; Kadnikova, E.N.; Liu, J.; Fréchet, J.M.J. Controlling the field-effect mobility of regioregular polythiophene by changing the molecular weight. *Adv. Mater.* **2003**, *15*, 1519–1522.
3. Zen, A.; Pflaum, J.; Hirschmann, S.; Zhuang, W.; Jaiser, F.; Asawapirom, U.; Rabe, J.; Scherf, U.; Neher, D. Effect of molecular weight and annealing of poly(3-hexylthiophene)s on the performance of organic field-effect transistors. *Adv. Funct. Mater.* **2004**, *14*, 757–764.
4. Schilinsky, P.; Asawapirom, U.; Scherf, U.; Biele, M.; Brabec, C.J. Influence of the molecular weight of poly(3-hexylthiophene) on the performance of bulk heterojunction solar cells. *Chem. Mater.* **2005**, *17*, 2175–2180.
5. Hosoi, K.; Mori, T.; Mizutani, T.; Yamamoto, T.; Kitamura, N. Effects of molecular weight on polyfluorene-based polymeric light emitting diodes. *Thin Solid Films* **2003**, *438–439*, 201–205.
6. Pate, K.R.; Lantz, A.; Dhawan, T.; Vo-Dinh, R.; Stiff-Roberts, A.D. Resonant infrared matrix-assisted pulsed laser evaporation of inorganic nanoparticles and organic/inorganic hybrid nanocomposites. *AIP Conf. Proc.* **2010**, *1278*, 813–823.
7. Pate, R.; Stiff-Roberts, A.D. The impact of laser-target absorption depth on the surface and internal morphology of matrix-assisted pulsed laser evaporated conjugated polymer thin films. *Chem. Phys. Lett.* **2009**, *477*, 406–410.
8. Pate, R.; McCormick, R.; Chen, L.; Zhou, W.; Stiff-Roberts, A. Rir-maple deposition of conjugated polymers for application to optoelectronic devices. *Appl. Phys. A* **2011**, doi:10.1007/s00339-011-6598-3.
9. Pate, R.; Lantz, K.R.; Stiff-Roberts, A.D. Tabletop resonant infrared matrix assisted pulsed laser evaporation of light emitting organic thin films. *IEEE J. Quantum. Elect.* **2008**, *14*, 1022–1030.
10. Pate, R.; Lantz, K.R.; Stiff-Roberts, A.D. Resonant infrared matrix-assisted pulsed laser evaporation of cdse colloidal quantum dot/poly[2-methoxy-5-(2'-ethylhexyloxy)-1,4-(1-cyano vinylene)phenylene] hybrid nanocomposite thin films. *Thin Solid Films* **2009**, *517*, 6798–6802.
11. Piqué, A.; McGill, R.A.; Chrisey, D.B.; Leonhardt, D.; Mslina, T.E.; Spargo, B.J.; Callahan, J.H.; Vachet, R.W.; Chung, R.; Bucaro, M.A. Growth of organic thin films by the matrix assisted pulsed laser evaporation (maple) technique. *Thin Solid Films* **1999**, *355–356*, 536–541.

12. Bubb, D.M.; Wu, P.K.; Horwitz, J.S.; Callahan, J.H.; Galicia, M.; Vertes, A.; McGill, R.A.; Houser, E.J.; Ringeisen, B.R.; Chrisey, D.B. The effect of the matrix on film properties in matrix-assisted pulsed laser evaporation. *J. Appl. Phys.* **2002**, *91*, 2055–2058.
13. Bubb, D.M.; Toftmann, B.; Haglund, J.R.F.; Horwitz, J.S.; Papantonakis, M.R.; McGill, R.A.; Wu, P.W.; Chrisey, D.B. Resonant infrared pulsed laser deposition of thin biodegradable polymer films. *Appl. Phys. A* **2002**, *74*, 123–125.
14. Bubb, D.M.; O'Malley, S.M.; Antonacci, C.; Simonson, D.; McGill, R.A. Matrix-assisted laser deposition of a sorbent oligomer using an infrared laser. *J. Appl. Phys.* **2004**, *95*, 2175–2177.
15. Toftmann, B.; Papantonakis, M.R.; Auyeung, R.C.Y.; Kim, W.; O'Malley, S.M.; Bubb, D.M.; Horwitz, J.S.; Schou, J.; Johansen, P.M.; Haglund, R.F. Uv and rir matrix assisted pulsed laser deposition of organic meh-ppv films. *Thin Solid Films* **2004**, *453–454*, 177–181.
16. Chrisey, D.B.; Piqué, A.; McGill, R.A.; Horwitz, J.S.; Ringeisen, B.R.; Bubb, D.M.; Wu, P.K. Laser deposition of polymer and biomaterial films. *Chem. Rev.* **2003**, *103*, 553–576.
17. Cristescu, R.; Mihaiescu, D.; Socol, G.; Stamatina, I.; Mihailescu, I.N.; Chrisey, D.B. Deposition of biopolymer thin films by matrix assisted pulsed laser evaporation. *Appl. Phys. A* **2004**, *79*, 1023–1026.
18. Caricato, A.; Leggieri, G.; Martino, M.; Vantaggiato, A.; Valerini, D.; Cretì, A.; Lomascolo, M.; Manera, M.; Rella, R.; Anni, M. Dependence of the surface roughness of maple-deposited films on the solvent parameters. *Appl. Phys. A* **2010**, *101*, 759–764.
19. Mercado, A.L.; Allmond, C.E.; Hoekstra, J.G.; Fitz-Gerald, J.M. Pulsed laser deposition vs. Matrix assisted pulsed laser evaporation for growth of biodegradable polymer thin films. *Appl. Phys. A* **2005**, *81*, 591–599.
20. Fitz-Gerald, J.M.; Jennings, G.; Johnson, R.; Fraser, C.L. Matrix assisted pulsed laser deposition of light emitting polymer thin films. *Appl. Phys. A* **2005**, *80*, 1109–1112.
21. Sellinger, A.T.; Martin, A.H.; Fitz-Gerald, J.M. Effect of substrate temperature on poly(methyl methacrylate) nanocomposite thin films deposited by matrix assisted pulsed laser evaporation. *Thin Solid Films* **2008**, *516*, 6033–6040.
22. Wyatt, P.J. Light scattering and the absolute characterization of macromolecules. *Anal. Chim. Acta* **1993**, *272*, 1–40.
23. Abdou, M.S.A.; Holdcroft, S. Solid-state photochemistry of π -conjugated poly(3-alkylthiophenes). *Can. J. Chem.* **1995**, *73*, 1893–1901.
24. Mirau, P.A. *A Practical Guide to Understanding the Nmr of Polymers*; Wiley-Interscience: Hoboken, NJ, USA, 2005.
25. Chen, T.-A.; Wu, X.; Rieke, R.D. Regiocontrolled synthesis of poly(3-alkylthiophenes) mediated by rieke zinc: Their characterization and solid-state properties. *J. Am. Chem. Soc.* **1995**, *117*, 233–244.
26. Rahman, M.H.; Chen, H.-L.; Chen, S.-A.; Chu, P.P.J. ^1H nmr spectroscopic study of the solution structure of a conjugated polymer. *J. Chin. Chem. Soc.* **2010**, *57*, 490–495.
27. Ram, M.K.; Sarkar, N.; Bertonecello, P.; Sarkar, A.; Narizzano, R.; Nicolini, C. Fabrication and characterization of poly[(2-methoxy-5-(2'-ethyl-hexyloxy)phenylene vinylene] (meh-ppv) langmuir-schaefer films and their application as photoelectrochemical cells. *Synth. Metals* **2001**, *122*, 369–378.

28. Collison, C.J.; Rothberg, L.J.; Treemanekarn, V.; Li, Y. Conformational effects on the photophysics of conjugated polymers: A two species model for meh-ppv spectroscopy and dynamics. *Macromolecules* **2001**, *34*, 2346–2352.
29. Verma, D.; Ranga Rao, A.; Dutta, V. Surfactant-free cdte nanoparticles mixed meh-ppv hybrid solar cell deposited by spin coating technique. *Solar Energy Mater. Solar Cells* **2009**, *93*, 1482–1487.
30. Jørgensen, M.; Norrman, K.; Krebs, F.C. Stability/degradation of polymer solar cells. *Solar Energy Mater. Solar Cells* **2008**, *92*, 686–714.
31. Brandrup, J.; Immergut, E.H.; Grulke, E.A. *Polymer Handbook*, 4th ed.; Wiley: New York, NY, USA, 1999.
32. Heffner, G.W.; Pearson, D.S. Molecular characterization of poly(3-hexylthiophene). *Macromolecules* **1991**, *24*, 6295–6299.

© 2012 by the authors; licensee MDPI, Basel, Switzerland. This article is an open access article distributed under the terms and conditions of the Creative Commons Attribution license (<http://creativecommons.org/licenses/by/3.0/>).